Supplemental Materials and Methods

Mass Spectrometry. Raw264.7 cells were plated in 15 cm plates and grown to confluence. Cells were washed with cold PBS and lysed. After centrifugation, supernatants were used for immunoprecipitation. Lysates were first precleared using mouse IgG coupled resin (for 2h) and then incubated with GRK2 antibody-coupled resin or mouse IgG resin as control (overnight at 4° C). Resin was washed four times with lysis buffer to remove any non-specific proteins, and then acid eluted and neutralized with Tris (pH 9). Samples were separated on SDS-PAGE gels and proteins were visualized using Coomassie stain. Unique bands present in the GRK2 IPs but not present in the control IPs were excised and submitted to Michigan State University Proteomics Facility for trypsinization and subsequent LC-MS/MS analysis. Data were analyzed using Scaffold program (Proteome Software, Inc).

Antibodies. Anti-BCL10 (sc-5611), anti-MALT1 (H300) (sc-28246), anti-MALT1 (B-12) (sc-46677), and anti-GRK2(C-15) (SC-562) were purchased from Santa Cruz Biotechnology. Anti-RELB (C1E4) (Cat. No 4922), anti-GAPDH (D16H11) (Cat. No 5174), anti-phospho-IκB (5A5, Ser32/36) (Cat. No 9246), anti-p65 (Cat No 3987s), anti-HDAC1 (10E2, HRP conjugate, cat No 59581S) were purchased from Cell Signaling Technology. Anti-CYLD (733) (Cat.No 43-700) was purchased from Invitrogen. Anti-Myc (4A6) (Cat. No 05-724) was purchased from EMD Millipore. Anti-mouse, rabbit and rat secondary antibodies were from Promega. Anti-HA affinity Matrix (3F10, Cat. No 11 815 016 001) and Anti-HA high affinity antibody (3F10, Cat.No 11 867 423 001) were from Roche.

Immunoprecipitation and immunoblotting. For immunoprecipitation, cells were rinsed in PBS, and lysed in buffer (150mM NaCl, 2mM EDTA, 10% glycerol, 1% Nonidet P-40, 20mM, Tris HCl, pH 7.4) containing protease and phosphatase inhibitors. Supernatants were incubated with

specified antibody for 1 hour at 4 °C followed by 30ul protein A/G beads overnight at 4 ° C with gentle rotation. Beads were then pelleted at 1000 rpm for 2 min and washed 3 times. Antibody-protein conjugates were removed from beads by boiling (5 min) and samples were then subjected to SDS-PAGE and immunoblotting.

MALT1-GRK2 binding. Purified recombinant full-length human GST-MALT1 (1 μg) or GST-BCL10 (1 μg) was incubated with purified recombinant full-length human GST-GRK2 (1 μg) in buffer (150mM NaCl, 2mM EDTA, 10% glycerol, 1% Nonidet P-40, 20mM, Tris HCl, pH 7.4) containing protease inhibitors for 1h at 4°C. The reaction mix was subjected to immunoprecipitation with specified antibody.

Lentivirus production and construction of stable cell lines. All recombinant lentiviruses were produced by transient transfection of 293Ta cells (Lenti-Pac 293Ta, Cat. No. CLv-PK-01; GeneCopoeia). For GRK2 shRNA lentivirus, subconfluent 293Ta cells (10cm plate) were co-transfected with 10 μg GRK2 shRNA or control shRNA, 5 μg pRRE, 2.5 μg pRSV, and 3 μg pVSV using lipofectamine 3000 (Invitrogen). For GRK2 ORF cDNA lentivirus, subconfluent 293Ta cells (10cm plate) were co-transfected with 10 μg lentiviral ORF cDNA clones for *GRK2/ ADRBK1* (EX-A0311-Lv103) with N-eGFP or empty vector control plasmid (Ex-NEG-Lv103), together with 5 μg pRRE, 2.5 μg pRSV and 3 μg pVSV using lipofectamine 3000 (Invitrogen). Lentivirus-containing supernatants of transfected cells were collected at 48h, the solution was filtered at 0.45 μM and concentrated using the Lenti-Pac™ lentivirus concentration solution (GeneCopoeia). Stable transfection of cells was established by lentiviral infection. Transfection efficiency was determined by flow cytometry and western blot analysis. Lentivirus-transduced cells were kept under puromycin selection at the indicated concentrations: Jurkat T (5 μg/ml), OCI- Ly1 and Ly7 (2 μg/ml), OCI-Ly3 and HBL1 (1 μg/ml).

GRK2 Knockout with CRISPR/Cas9 system. The Jurkat and OCI-LY3 GRK2 knockout cell lines were custom-made by Genscript. gRNAs targeting the RGS region of GRK2 were designed using the CCTOP gRNA design tool (https://crispr.cos.uni-heidelberg.de/) along with CRISPRater which together determined the most efficient and specific guiding RNAs. Guide RNA sequence TCAGTGGCACTCTTCGAGAA with highest cleavage efficiency was used to generate gRNA-Cas9 plasmid or the gRNA-Cas9 ribonucleoprotein reagent. Jurkat cells were electroporated with gRNA-Cas9 plasmid and OCI-Ly3 cells were electroporated with gRNA-Cas9 RNP following Genscript user manual and monoclonal cell populations were generated by limiting dilution. Targeted disruption of GRK2 was confirmed by Sanger sequencing. Allelic analysis was carried out using Sanger sequencing and Tracking of Indels by decomposition (TIDE) (available at https://tide.nki.nl/).

GRK2-deficient B cells. To generate bone marrow chimeras, BM cells from Mb1cre- $GRK2^{fl/+}$ or Mb1cre+ $GRK2^{fl/fl}$ mice (provided by Dr. Jason Cyster, UCSF) were transferred into irradiated C57BL/6(B6) (NCI) recipients. Chimeras were analyzed at 8-12 weeks after reconstitution. Spleens and pLN were isolated from Mb1cre- $GRK2^{fl/+}$ or Mb1cre+ $GRK2^{fl/fl}$ mice and primary B cells were enriched with EasySep™ Mouse Pan-B Cell Isolation Kit (STEMCELL technologies).

Cell proliferation assay. Cell numbers were counted using Vi-cell cell counter (the trypan blue dye exclusion method) from Beckman Coulter.

Luciferase assay. HEK-293T cells were transfected with varying amounts of plasmid expressing the indicated proteins, in combination with an NF-κB-responsive luciferase reporter plasmid (pNF-κB-luciferase) (Stratagene, La Jolla, CA), and a *Renilla* plasmid (phRL-TK) (Promega, Madison, WI) was used to control for transfection efficiency. In each experiment, the total amount of DNA in each sample was kept constant by supplementation with the appropriate empty parental

expression vector. 24h post-transfection, the activities of Firefly and Renilla luciferase were measured using the Dual-luciferase reporter assay system (Promega), according to the manufacturer's instructions. The data represent relative Firefly luciferase activity normalized to Renilla luciferase activity and are representative of the independent experiments in triplicate. Data are presented as mean ±SEM. Jurkat T cells were transfected by electroporation using a Gene-Pulser (Bio-Rad) at 250 V and 960 μF and cultured overnight before stimulation.

ELISA. Cytokine concentrations in culture supernatants were measured by ELISA. Human IL-2 (431804), IL-6 (430504), Il-10 (430604) ELISAs (BioLegend) were performed according to the manufacturer's protocols.

Nuclear protein extraction and NF-κB (p65) Transcription Factor Assay. After experimental exposures, $7.5x10^6$ cells were spun down, supernatant removed, and rinsed twice in PBS. Following centrifugation, the cell pellet was resuspended in 500ml buffer A (10mM HEPES, pH 7.9, 0.1mM EDTA, 0.1mM EGTA, 10mM KCL and protease inhibitors, 1.0mM DTT and 1% NP-40 added fresh) to lyse the cells. After a 20 minutes incubation on ice, the lysate was centrifuged at 13,000g for 5 min at 4ºC to pellet the nuclei. The cytosolic supernatant was removed and saved while the nuclei pellet was washed 3x by adding 250ml of buffer A and centrifuged as previous. After washing, the nuclei pellet was resuspended in 15ml buffer C (20mM HEPES, pH 7.9, 0.42M NaCl, 1.0mM EDTA, 0.1mM EGTA, with DTT and protease inhibitors added fresh) and samples were vortexed and shaken at 4ºC for 15 min. After a 10 min centrifugation at 13,000g, 4ºC, the nuclear protein supernatant was removed and mixed with 22.5ml of buffer D (20mM HEPES, pH 7.9, 20% v/v glycerol, 0.1M KCl, 1.0mM EDTA, 0.1mM EGTA with 1% NP-40, DTT and protease inhibitors added fresh). Nuclear protein concentration was determined by Coomassie dye-based assay (Pierce, Rockford, Il) comparing samples to a BSA standard curve. 5 mg of

nuclear protein was used in NFkB (p65) ELISA Kit (Rockland Antibodies and Assays, Cat# KAA065). Duplicate technical reps of biological triplicates were assayed according to manufacturer's directions. Data was analyzed by 2way ANOVA with a Tukey's multiple comparison post-test (Graphpad Prism) and data is presented is one of 3 different experiments.

Immune cell clustering and proliferation assay. HBL1 cells with control GFP or GFP-GRK2 were seeded into 6-well plates in duplicate and placed into the IncuCyte ZOOM instrument (Essen Bioscience). IncuCyte ZOOM software was utilized to schedule repeat scanning every 2 hours. Immune cell proliferation was quantified by IncuCyte software using the confluence algorithm. To quantify immune cell clustering, size filters are applied to the confluence algorithm to identify aggregates with a minimal area of 1500 μm^2 and a maximal eccentricity of 0.95. Results are expressed as the number of clusters per square millimeter.

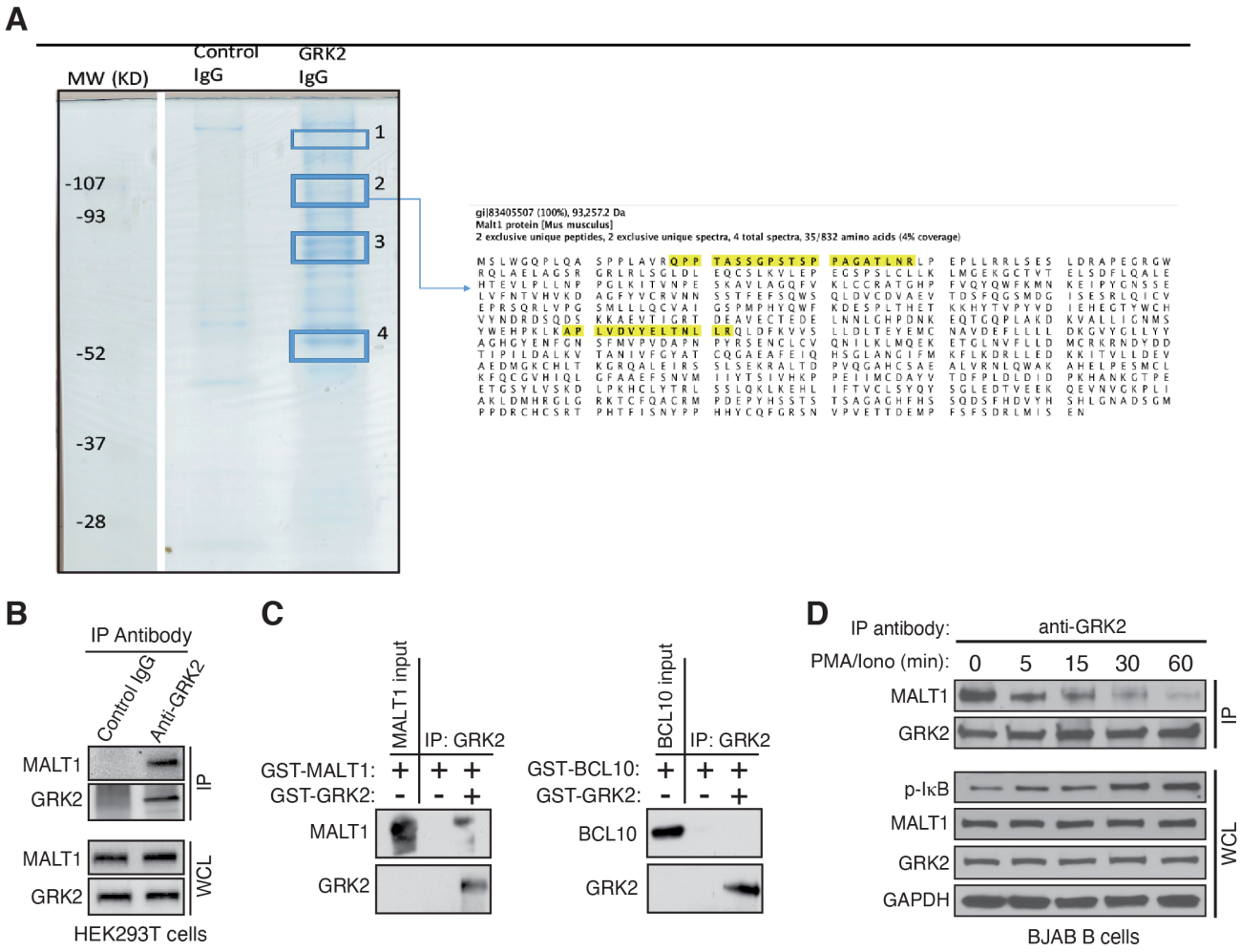

Supplemental Figure 1. Identification of GRK2 as a novel MALT1 binding partner. (**A**) GRK2 IP coupled with mass spectrometry identified MALT1 as a co-immunoprecipitated protein. Raw264.7 cell lysates were precleared with control-IgG-coupled aminolink resin for 2 hours, then immunoprecipitated with either GRK2 or control IgG antibody-coupled resin overnight. Eluted proteins were run on SDS-PAGE and visualized using coomassie stain. Unique bands from GRK2 IP were excised and submitted for trypsin digestion and mass spectrometry analysis (LS-MS-MS). Peptides identified by mass spectrometry, spanning the MALT1 protein, are shown highlighted in yellow. (**B**) Endogenous MALT1 and GRK2 interact in HEK 293T cells. Co-IP of MALT1 and GRK2 was demonstrated by western blot. (**C**) Reverse pull-down with purified recombinant proteins confirmed that GRK2 directly interacts with MALT1 but not BCL10. (**D**) AgR stimulation leads to GRK2/MALT1 dissociation in BJAB B-cells. All blots shown are representative of at least two seperate experiments.

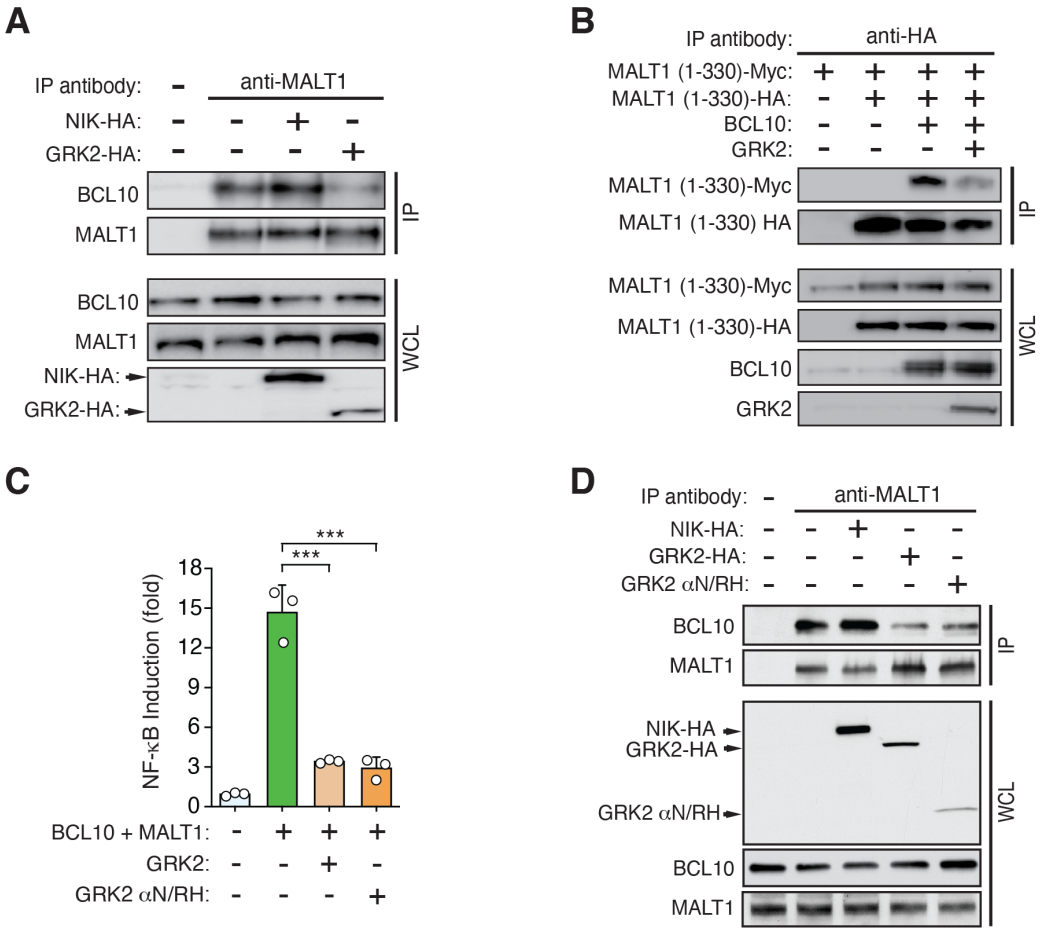

Supplemental Figure 2. GRK2 inhibits MALT1 interaction with BCL10 and MALT1 oligomerization, and GRK2 αN/RH (AA 1-173) is as effective as full-length (FL) GRK2 in inhibiting NF-κB activation and MALT1/BCL10 interaction. (**A**) GRK2 inhibits BCL10 interaction with MALT1. HA-tagged GRK2 or control protein, HA-NIK, were expressed in HEK293T cells and the Co-IP of endogenous BCL10 with MALT1 was assessed by western blot (n=3). GRK2 disrupts the BCL10/MALT1 interaction whereas the unrelated control protein, NIK, does not. (**B**) GRK2 inhibits MALT1 oligomerization. HA-tagged and Myc-tagged MALT1 (AA1-330) were transfected as indicated together with/without BCL10. The impact of GRK2 on BCL10 dependent MALT1 oligomerization was analyzed by western blot (n=3). (**C**) GRK2 αN/RH (AA 1-173) is as effective as FL GRK2 in inhibiting BCL10/MALT1-induced NF-κB luciferase reporter activity (n=3). ***P<0.001, by one-way ANOVA, followed by Tukey's multiple comparison test. (**D**) GRK2 αN/RH (AA 1-173) is as effective as FL GRK2 in inhibiting BCL10 interaction with MALT1. HA-tagged GRK2 (FL or GRK2 αN/RH) or control protein, HA-NIK, were expressed in HEK293T cells and the Co-IP of endogenous BCL10 with MALT1 was assessed by western blot (n=3).

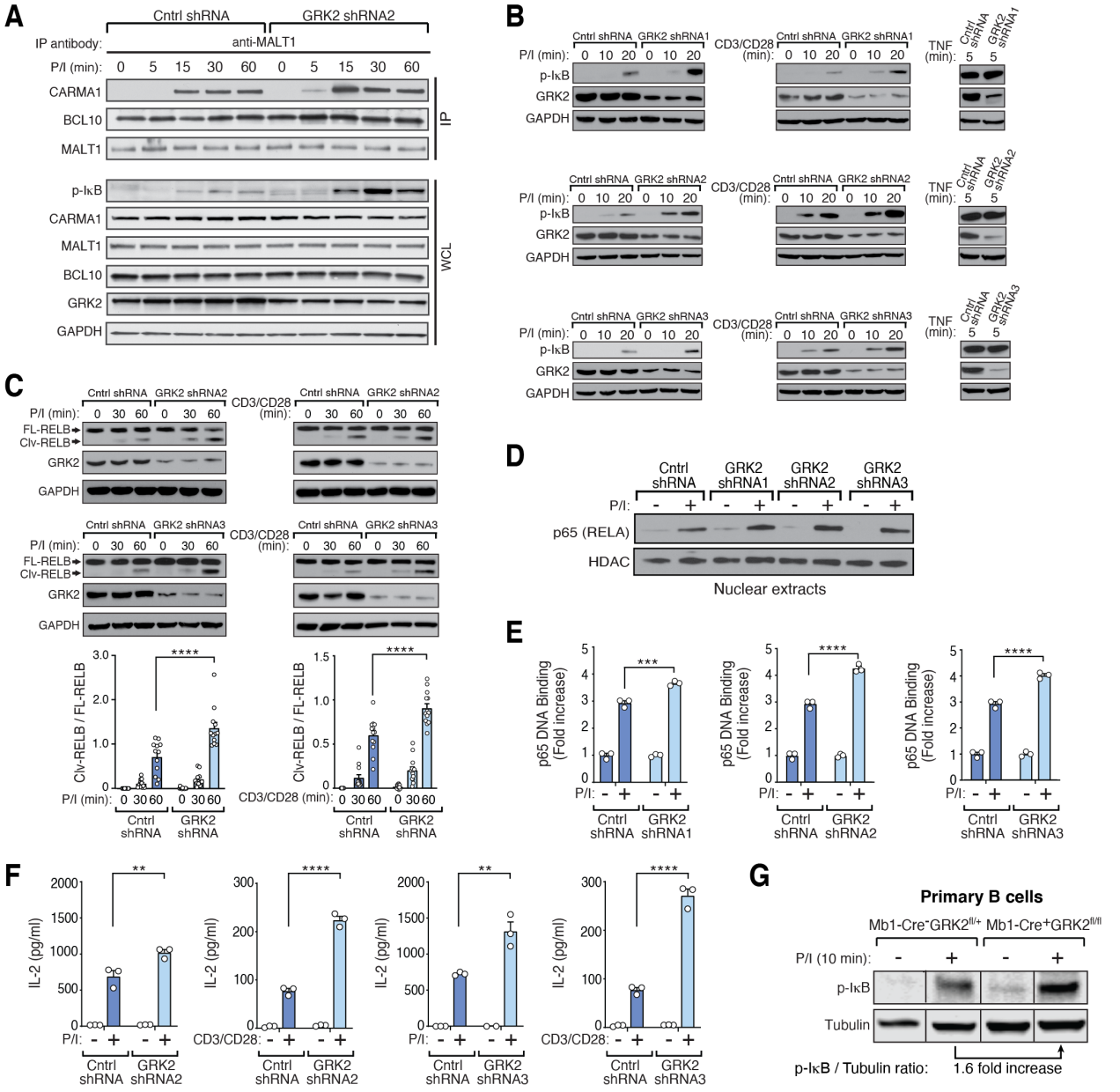

Supplemental Figure 3. GRK2 attenuates AgR stimulation induced CBM complex formation, MALT1 protease activity, NF-κB activation, and IL-2 production. (**A**) Knockdown (KD) of GRK2 in Jurkat T-cells enhances P/I-induced CBM complex formation in an additional Jurkat GRK2 KD clone infected by lentiviral GRK2 shRNA targeting a different region of GRK2 (GRK2 shRNA2). Jurkat T-cells were subjected to knockdown with either control or GRK2 shRNA lentivirus and then treated with/without P/I. Binding of BCL10 and CARMA1 to immunoprecipated MALT1 were examined (n=3). (**B**) GRK2 KD in Jurkat T-cells was performed using three distinct shRNAs targetting different regions of GRK2. In each case, knockdown of GRK2 leads to enhanced P/I (left panel) or anti-CD3/CD28 (middle panel) but not TNF(right panel) induced IκB phosphorylation. (**C**) GRK2 KD leads to increased cleavage of RELB in response to P/I (left panel) or anti-CD3/CD28 (right panel) stimulation in two additional Jurkat GRK2 KD clones (GRK2 shRNA2 and GRK2 shRNA3). Quantification is shown below (n=3-4 per shRNA clone x 3 individual shRNAs). ****P<0.0001. (**D**) GRK2 KD leads to enhanced p65 nuclear translocation after P/I stimulation. Nuclear extracts were made and analyzed by western blot. HDAC was used as a control for nuclear protein. (**E**) GRK2 KD leads to enhanced p65 DNA binding after P/I stimualtion. Nuclear extracts were made from P/I treated control and GRK2 KD cells and analyzed using non-radioactive EMSA kit (n=3). ***P<0.001, ****P<0.0001. (**F**) GRK2 KD leads to enhanced IL-2 production in Jurkat T- cells. Cells were treated as indicated for 24 hours and IL-2 in supernatants was measured by ELISA (n=3). *P<0.05, ***P<0.001,****P<0.0001. (**G**) GRK2 knockout in primary B cells enhances P/I-induced IκB phosphorylation. Bone marrow cells of Mb1-Cre-GRK2$^{fl/+}$ or Mb1-Cre+GRK2$^{fl/fl}$ mice were transfered to irradiated C57BL/6 (B6) recipients. Chimeras were analyzed 8-12 weeks after reconstitution. Primary B cells were isolated from spleens and treated with P/I for indicated time (n=2). Vertical lines are included in the figure to indicate that lanes were run on the same gel but were non-contiguous. Statistical significance for panels C, E, and F was evaluated by two-way ANOVA, followed by Tukey's multiple comparison test.

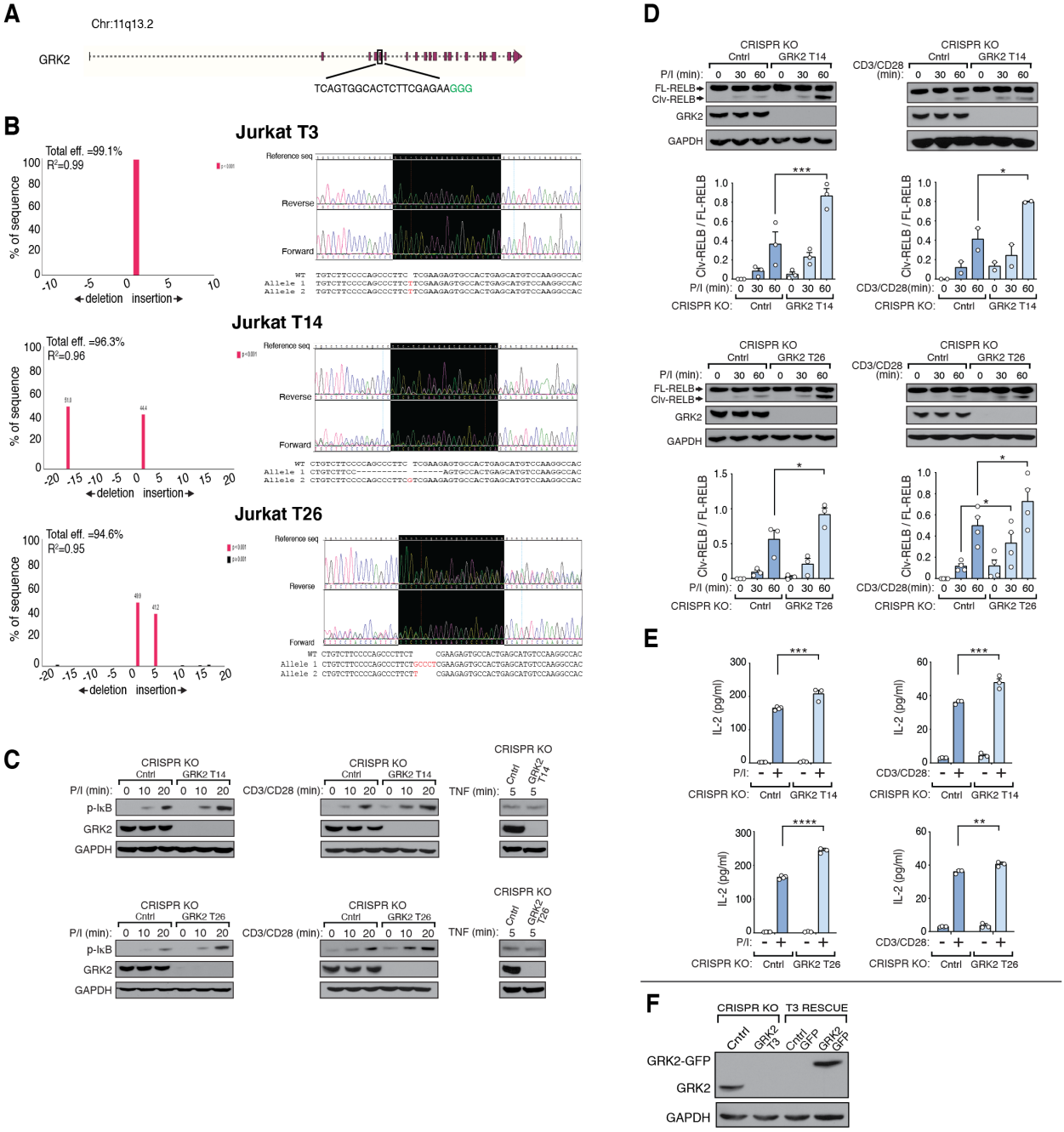

Supplemental Figure 4. Targeted knockout (KO) of GRK2 leads to enhanced MALT1-dependent activities in Jurkat T-cells (**A**) Overview schematic of the Cas9/gRNA target site. Genomic coordinates are shown on the left. The gRNA-targeting sequence is shown, and the PAM sequence is labeled in green. (**B**) TIDE analysis (left), chromatogram sequence alignment and allelic analysis of the gene editing activity (right), around the GRK2 target site of the clonally expanded populations (T3, T14 and T26) are shown. Sanger sequencing of both the forward and reverse strand is shown. (**C**) GRK2 KO leads to increased P/I-(left panels) or anti-CD3/CD28-(middle panels) but not TNF-(right panels) induced IκB phosphorylation in additional Jurkat T-cell clones (T14 and T26). GRK2 KO was confirmed by western blot. Blots are representative of at least 3 experiments. (**D**) Cleavage of RELB induced by P/I (left panel) or anti-CD3/CD28 (right panel) was enhanced in additional GRK2 KO Jurkat T-cell clones (T14 and T26). Densitometric quantification was performed using Alphaview software (n=2-4). Clv, cleaved; FL, full-length. *P<0.05, ***P<0.001. (**E**) IL-2 production was enhanced in additional GRK2 KO Jurkat T-cell clones (T14 and T26). Cells were treated with/without P/I or anti-CD3/CD28 for 24 hours and IL-2 in the supernatant was measured by ELISA. Results are expressed as the mean ± SEM (n=3-4). **P<0.01, ***P<0.001, ****P<0.0001. (**F**) GRK2 rescue in GRK2 KO Jurkat T-cell clone T3 was achieved using lentiviral WT GRK2-GFP. Statistical significance for panels D and E was evaluated by two-way ANOVA, followed by Tukey's multiple comparison test.

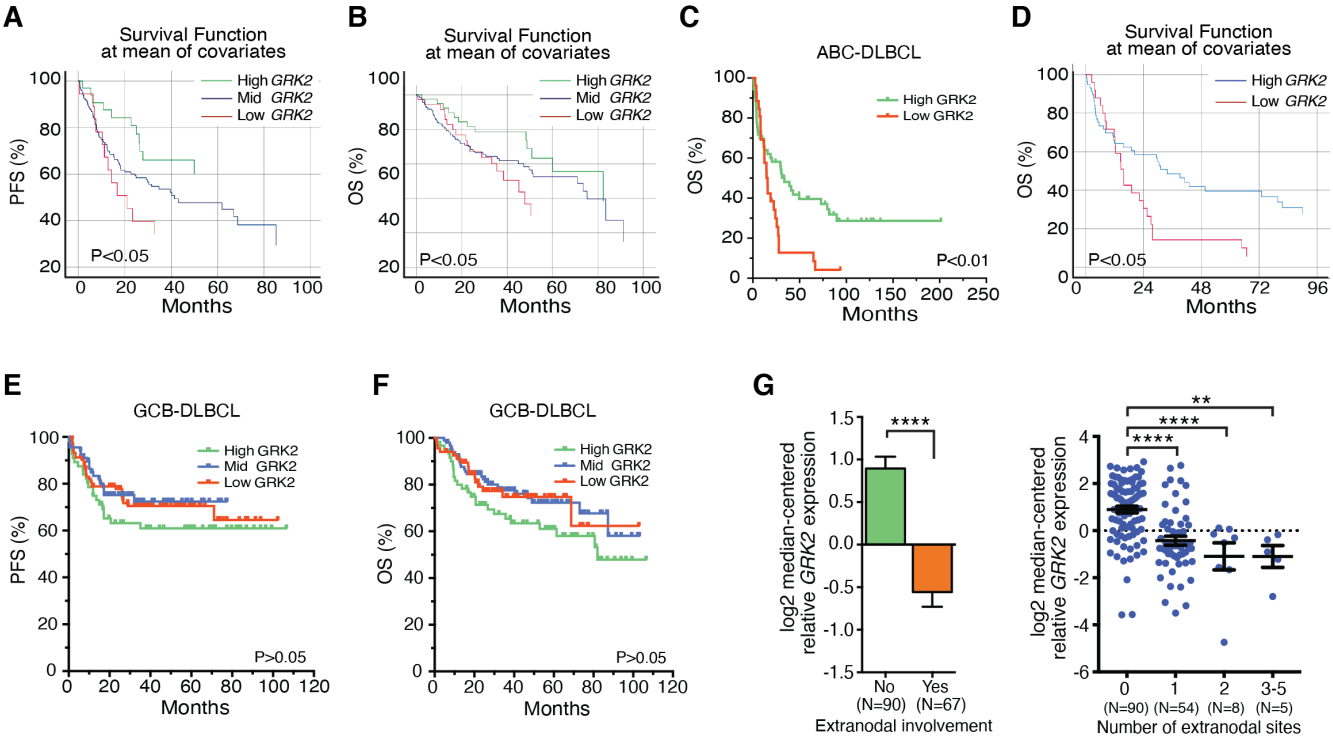

Supplemental Figure 5. Additional bioinformatic analyses related to *GRK2* expression in human DLBCL. (**A**,**B**) Kaplan-Meier plots for PFS (**A**) and OS (**B**) at the mean of sampled covariates show that *GRK2* is an independent risk factor for mortality. Data for panels A and B were accessed from same public repository (GSE31312) as in **Figure 6C** and **D** and then analyzed by multivariate Kaplan Meier analysis, controlling for age and gender. (**C**) OS rates of ABC-DLBCL patients are significantly lower in patients with low *GRK2* as compared to high *GRK2*. Overall survival curves were stratified by high and low *GRK2* expression values from an additional dataset (GSE4732). Statistical significance was evaluated using Log-rank test. (**D**) The Kaplan Meier plots of dataset (GSE4732) at the mean of sampled covariates confirms that *GRK2* is a independent predictor of OS (P<0.05) in ABC-DLBCL patients. Data were analyzed by multivariate Kaplan Meier analysis as in (A) and (B). (**E**,**F**) Rates of PFS (**E**) and OS (**F**) of GCB-DLBCL patients are not different between GRK2 high and low groups. Expression of GRK2 was stratified into high, mid and low ranges using dataset-wide quartile cutoffs (high 25%, mid 50%, low 25%). Statistical significance was evaluated using Log-rank test. Data were accessed from the same public repository as in **Figure 6C** and **D** (GSE31312). (**G**) Low *GRK2* expression in ABC-DLBCL is associated with extranodal spread (left panel). Further, the number of extranodal sites involved correlates with increasingly lower *GRK2* levels (right panel). *GRK2* expression levels were obtained from microarray data available in public repository GSE10846. **P<0.01, ****P<0.0001, by MANOVA.

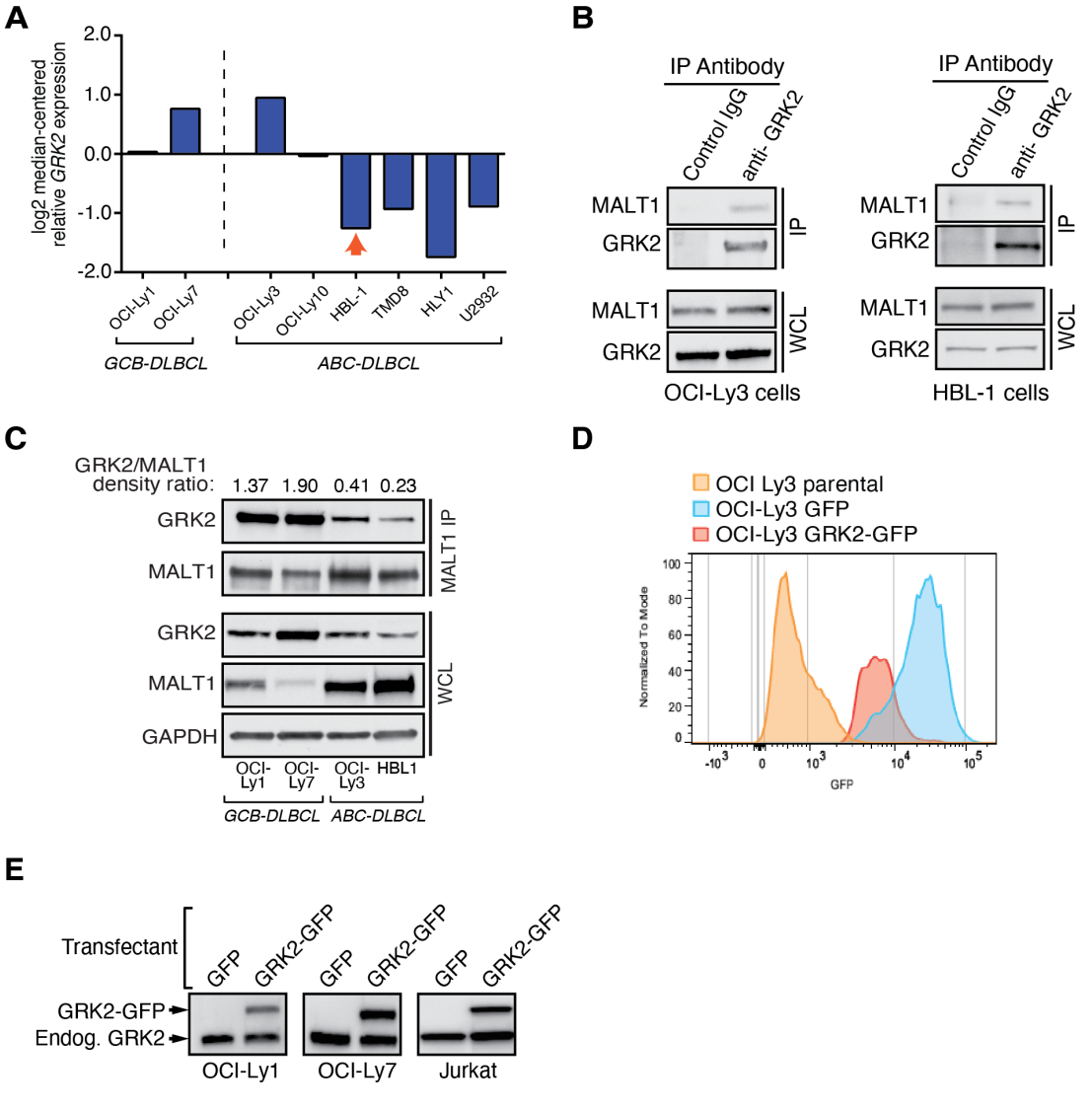

Supplemental Figure 6. GRK2 expression and endogenous MALT1 and GRK2 interaction in GCB and ABC-DLBCL lines. (**A**) An independent dataset was used to confirm the markedly low GRK2 mRNA level in HBL1 cells. cDNA microarray data were retrieved from the public repository (GSE57083) and analyzed. (**B**) Endogenous MALT1 and GRK2 interact in OCI-Ly3 and HBL1 cells. Co-IP of MALT1 with GRK2 was demonstrated by western blotting. Blots are representative of 3 separate experiments. (**C**) Relatively less binding of GRK2 to MALT1 was found in ABC-DLBCL as compared to GCB-DLBCL cell lines. CO-IP of MALT1 and GRK2 was demonstrated by western blot (n=3). The amount of GRK2 associated with immuno-precipited MALT1 was quantified (numbers shown above the blots). (**D**) GRK2-GFP was effectively expressed in OCI-Ly3 cells infected with lentivirus, as detected by flow cytometry. Data are representative of 3 independent experiments. (**E**) GRK2-GFP was efficiently expressed in two GCB-DLBCL lines (OCI-Ly1 and OCI-Ly7) and in Jurkat T-cells (n=3). Stable cell lines were made using the same lentivirus as was used in ABC-DLBCL cells.

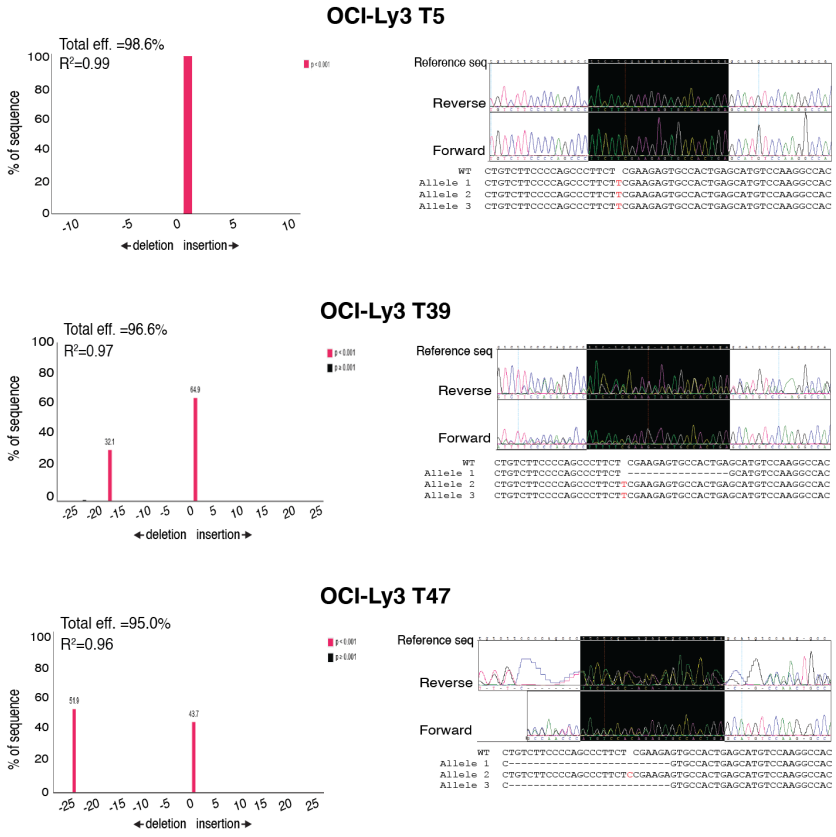

Supplemental Figure 7. TIDE analysis (left), chromatogram sequence alignment and allelic analysis of the gene editing activity (right), around the GRK2 target site of the clonally expanded populations (T5, T39 and T47) of OCI-Ly3 cells are shown. Sanger sequencing of both the forward and reverse strand is shown.

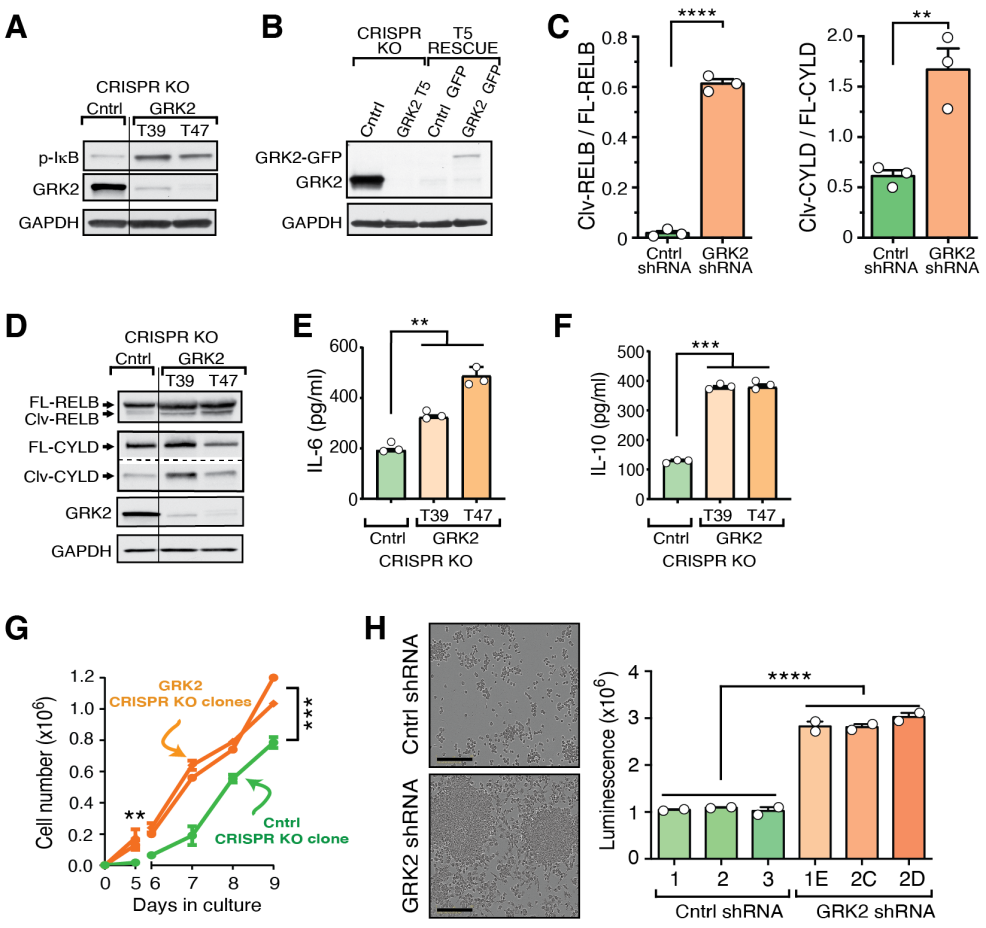

Supplemental Figure 8. Targeted knockout (KO) of GRK2 leads to enhanced MALT1 activity, MALT1-dependent cytokine secretion and proliferation in ABC-DLBCL cell line OCI-Ly3. (**A**) GRK2 KO leads to increased basal IκB phosphorylation in additional OCI-Ly3 clones (T39 and T47). OCI-Ly3 cells with GRK2 KO were made using Cas9/gRNA. GRK2 KO was confirmed by western blot. Blots are representative of at least 3 experiments. A vertical line is included in the figure to indicate that lanes were run on the same gel but were non-contiguous. (**B**) Rescue of GRK2 was achieved using lentiviral WT GRK2-GFP in GRK2 KO OCI-Ly3 clone T5 (n=3). (**C**) Densitometric analysis of RelB and CYLD cleavage using Alphaview for Figure 8B**.** Results are expressed as the mean ± SEM (n=3). **P<0.01, ****P<0.0001. (**D**) GRK2 KO leads to increased cleavage of RELB and CYLD in additional OCI-Ly3 clones (T39 and T47). Blots shown are representative of n=3. A vertical line is included in the figure to indicate that lanes were run on the same gel but were non-contiguous. Clv, cleaved; FL, full-length. (**E and F**) GRK2 KO leads to increased IL-6 and IL-10 production in additional OCI-Ly3 clones (T39 and T47). IL-6 and IL-10 secretion were determined by ELISA (n=3). **P<0.01, ***P<0.001. (**G**) GRK2 KO leads to increased proliferation in additional OCI-Ly3 clones (T39 and T47). Results are expressed as the mean ± SEM (n=3). ***P<0.001 by two way ANOVA and Dunnett's multiple comparisons test (significance for the end time points is shown). (**H**) shRNA-mediated GRK2 knockdown leads to increased cellular aggregation and adhesion of OCI-Ly3 cells. Cells were cultured for 72 hours without agitation. Attached cells were imaged using the IncuCyteZOOM instrument (x20) after unattached cells were carefully removed with the culture supernatant. Scale bars: 200μm. Cells attached to the bottom of the culture dish were quantified using luminescence detection. Results are expressed as the mean ± SEM, ****P<0.0001. Control clones (1, 2, and 3) and GRK2 KD clones (1E, 2C, and 2D) were analyzed separately (total of n=6 for both control and for GRK2 KD). Statistical significance for panels C, E, F, and H was evaluated by unpaired, two-tailed Student's T test.

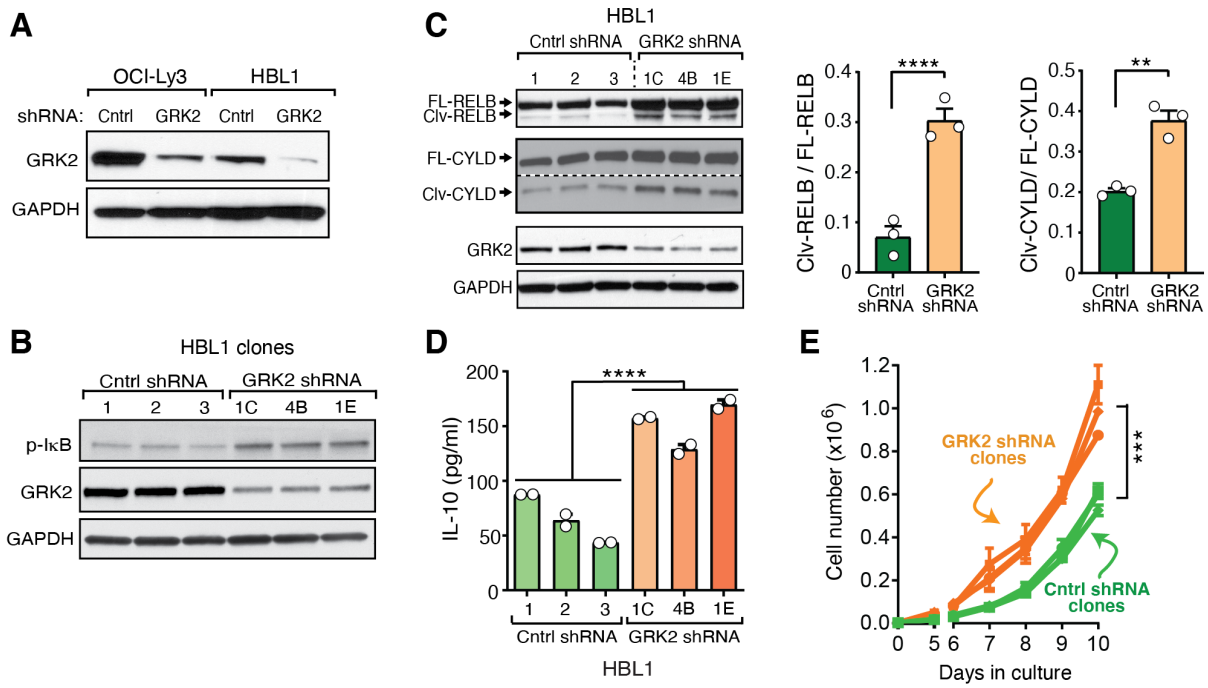

Supplemental Figure 9. Knockdown of GRK2 results in enhanced MALT1-dependent activity in another ABC-DLBCL cell line (HBL1). (**A**) As with OCI-Ly3 cells, GRK2 can be targeted for knockdown by shRNA in HBL1 cells. (**B**) GRK2 knockdown leads to increased basal IκB phosphorylation in HBL1 cells. Stable HBL1 cells with GRK2 knockdown were made using shRNA-encoding lentivirus (3 GRK2 knockdown clones are shown; 1C, 4B, and 1E). GRK2 knockdown was confirmed by western blotting. Blots are representative of at least 3 experiments. (**C**) Stable knockdown of GRK2 in HBL1 cells results in increased cleavage of RELB and CYLD. Blots shown are representative of three experiments. Densitometric analysis of cleavage using Alphaview is shown on the right (n=3). **P<0.01, ****P<0.0001 by unpaired, two-tailed Student's T test. Clv, cleavage; FL, full-length. (**D**) GRK2 knockdown leads to increased IL-10 production in HBL1 cells. IL-10 secretion was determined by ELISA. Control clones (1, 2, and 3) and GRK2 KD clones (1E, 2C, and 2D) were analyzed separately (total of n=6 for both control and for GRK2 KD). ****P<0.0001, by unpaired, two-tailed Student's T test. (**E**) GRK2 knockdown leads to increased proliferation of HBL1 cells (n=3). Two-way ANOVA and Sidak's multiple comparison test were performed to show proliferation differences between the GRK2 KD and control groups. ***P <0.001.